ASTRONOMY & ASTROPHYSICS
SUPPLEMENT SERIES

Astron. Astrophys. Suppl. Ser. **142**, 225–238 (2000)

A deep echelle survey and new analysis of diffuse interstellar bands⋆,⋆⋆

S.Ó. Tuairisg[1,2,3], J. Cami[4], B.H. Foing[2], P. Sonnentrucker[2], and P. Ehrenfreund[1]

[1] Leiden Observatory, P.O. Box 9513, 2300 RA Leiden, The Netherlands
[2] Solar System Division, ESA Space Science Department, ESTEC/SO, 2200 AG Noordwijk, The Netherlands
[3] Department of Physics, National University of Ireland Galway, Ireland
[4] Astronomical Institute "Anton Pannekoek", University of Amsterdam, Kruislaan 403, 1098 SJ Amsterdam, The Netherlands

Received October 30, 1998; accepted November 10, 1999

Abstract. We report a deep survey of diffuse interstellar bands (DIBs) between 3906 Å and 6812 Å under consistent observing conditions toward three very reddened and five unreddened stars. BD+63° 1964's line-of-sight was shown to present exceptional DIB enhancement in number as well as in strength. The early spectral type of the star and the use of spectra of an unreddened comparison star of the same spectral type allowed to limit stellar line residuals. Using careful reduction and analysis methods we discovered 60 new DIBs which are confirmed in the reddened targets HD 183143 and BD+40° 4220. We detected 25 possible DIBs which still await further confirmation, but we did not detect or confirm 28 previously reported DIBs. The present survey with 226 confirmed DIBs, measured in three targets allows a detailed and homogeneous statistical analysis on the distribution of DIB widths and intensities.

Key words: ISM: general — ISM: molecules

1. Introduction

Superimposed on the extinction curve are a huge number of absorption lines, the diffuse interstellar bands (DIBs). The identification of the DIB carriers remains an important problem in astronomy. The current number of ∼200 DIBs is still increasing, suggesting that more than 400 DIBs down to the confusion limit could be detected in the interstellar medium. The development of DIB research in recent years indicates that most DIB carriers could be large carbon-bearing molecules which reside ubiquitously in the interstellar gas (see Herbig 1995 for a review, Salama et al. 1996). The first detection of substructures in the profile of several DIBs indicated the molecular nature of some DIB carriers (Sarre et al. 1995; Ehrenfreund & Foing 1996). Foing & Ehrenfreund (1994, 1997) observed two DIBs at 9577 and 9632 Å as first evidence for C_{60}^+, the largest molecule ever detected in space. A survey of DIB correlations over 4000 Å showed that most of the DIB carriers are undergoing photo-ionization and that all measured DIBs do originate from different carriers (Cami et al. 1997).

Recently many laboratories, theoreticians and observational astronomers showed combined efforts to solve the long-standing mystery of the DIBs and to identify their carriers. The spectra of PAH and fullerene cations, measured in a Neon matrix, carbon chains measured in the gas phase and theoretical calculations of the non-linear H_2-DIB model have all shown some coincidences with some diffuse bands (see Salama et al. 1996; Foing & Ehrenfreund 1997; Freivogel et al. 1994; Sorokin et al. 1996; Ubachs et al. 1997; Tulej et al. 1998).

Another approach to identify the DIB carriers is to study the complete DIB spectrum in different interstellar and circumstellar regions and to relate the line-of-sight conditions directly to the formation/evolution and destruction properties of DIB carrier molecules. Additional observations of spectral molecular features such as CH, CH^+, CN (as well as atomic lines CaI, CaII, NaI) reveal variations of physical parameters of the interstellar environment and can constrain the chemistry, ionization balance, metallicity and electron density in the circumstellar and interstellar environment. To define those parameters and to relate them to the DIB behaviour in the same region allows another view on the nature of the DIB carriers.

Observations show currently up to ∼200 DIBs in dense and cold environments as well as in UV dominated

Send offprint requests to: P. Ehrenfreund

⋆ Based on observations at Observatoire Haute Provence with the spectrograph ELODIE.

⋆⋆ Figures 6 to 40 are only available in electronic form at http://www.edpsciences.org

regions. Their central wavelength is extremely constant. The band strength of the strongest DIBs (such as the 5780 and 5797 Å DIBs, which are measured towards more than 200 sources) does not change by more than a factor ∼2. The relative DIB strength, $W/E_{(B-V)}$, seems to reflect an interplay between ionization and recombination/destruction of the DIB carrier molecules. Even the high resolution profile of the 6613 Å DIB, which shows a characteristic triple peak, displays only slight changes in different environments.

A new reference target for DIB studies was recently detected, which shows the strongest DIBs ever measured and allows to define the DIBs in several categories which respond in totally different ways to the local environment (Ehrenfreund et al. 1997). We discuss the optical survey towards the star BD+63° 1964 which led to the detection of 60 new DIBs. We present the complete DIB spectrum between 3906 and 6812 Å of BD+63° 1964 and two other heavily reddened reference targets, HD 183143 and BD+40° 4220, and discuss the statistics of the confirmed DIBs.

2. Previous DIB surveys

In recent years the number of known DIBs has experienced considerable growth. This rapid increase is due to the improvement of CCDs and higher resolution instruments in the optical range. Herbig (1975) announced a total of 39 identified diffuse interstellar bands between 4400 and 6850 Å. In high signal to noise scans of reddened stars Herbig (1988) reported the discovery of 29 new lines between 6767 and 6862 Å. In a later publication Herbig & Leka (1991) added 22 more DIBs to an ever-growing list. Most of these surveys concentrated on the star HD 183143. It was clear at this point that the main barriers in revealing more DIBs was instrumental. To date, the largest DIB survey was reported by Jenniskens & Désert (1994). This survey included all the previously identified DIBs, and yet higher resolution than before resulted in the identification of more DIBs. The survey, from 3800 Å to 8680 Å, revealed a total of 229 DIBs. This list included 153 certain DIBs as well as 76 probable and questionable DIBs. The survey covered a wider wavelength range than the present one of BD+63° 1964, but some regions of the spectrum were omitted in their data. A subsequent smaller survey, but using a resolution of 60 000 concentrated on several different wavelength regions (Krelowski et al. 1995). These were mostly ∼80 Å windows centred at 5790 Å, 5915 Å, 6010 Å, 6250 Å, 6400 Å and 6665 Å. This survey resulted in the tentative identification of 42 weak DIBs. These DIBs were labeled either as certain or as doubtful DIBs.

The total number of diffuse interstellar bands identified in the wavelength range 3800 Å to 6815 Å until now is 184, 103 of these being classified as "certain" by Jenniskens & Désert (1994). What makes this present survey of these three reference targets both unique and necessary is: (i) the enhancement of narrow DIBs in BD+63° 1964, mentioned below, enabling us to confirm many of the weaker DIBs already reported, as well as to discover many new DIBs. (ii) Never before has there been a survey of diffuse interstellar bands from 3980 Å to 6820 Å in one echelle spectrum. To cover a wide wavelength range it was necessary for previous surveys to take a number of different exposures of the same stars over a period of several months. This created numerous complications such as different seeing and telluric conditions, and calibration drifts, which do not arise in our data. We have analysed a consistent, deep exposure over the desired wavelength range of the star BD+63° 1964 which shows, to date, the strongest DIBs ever measured. (iii) We measured a number of unreddened targets to optimize instrumental, telluric and stellar line corrections. (iv) The detected DIB candidates have been checked for confirmation in deep spectra of two very reddened targets, HD 183143 and BD+40° 4220, which have very different spectral types and rotation.

3. Observations and data reduction

3.1. ELODIE spectrograph performances

Observations were obtained on July 24th and November 8th, 1995 at the Observatoire de Haute Provence (OHP). We used the 1.93 m telescope, equipped with the spectrograph ELODIE, which is a fiber-fed echelle spectrograph, covering the wavelength range from 3906 to 6811 Å with a resolution of ∼ 42 000 (Baranne et al. 1996). The fibres are POLYMICRO fibres with a diameter of 100 μm. The grating used is a 408×102 mm echelle grating with 31 grooves/mm and a $\theta = 76°$ blaze angle. The dispersion crossing is done with two optical components, a 40° flint prism and a 8.63° crown grism with 150 grooves/mm. The combination results in a constant interorder spacing over the 67 spectral orders. The detector is a back-illuminated Tk1024 CCD with 24 μm pixels, cooled to 183 K. At a readout of 100 μs/pixel the typical readout noise is 8.5 e^-. The CCD has a linear response up to 100 000 e^-.

The preliminary reduction of the ELODIE data was performed on-line at the observatory. The normal CCD reduction procedure was carried out, incorporating the correction of bad-pixels and cosmic rays, and the subtraction of the bias and dark current. No systematic post-reduction deglitching was applied except for very obvious spikes.

3.2. The program stars and optimal reduction

In addition to BD+63° 1964, observations of three different standard stars were performed during the same night. Table 1 summarises the physical and observational characteristics of all the stars used in this survey. HD 37128,

Table 1. Physical and observational parameters for the program stars used in the DIB survey. The radial and rotational velocities were determined from the spectra

Target	BD+63° 1964	HD 183143	BD+40° 4220	HD 32630	HD 37128	HD 205021	HD 164353	HD 188209
V magnitude	8.6	6.86	9.05	3.20	1.70	3.19	3.97	5.62
Spectral Type	B0 II	B7Iae	O7e	B3 V	B0 I	B1 IV	B5Ib	O9.5Ib
$E_{(B-V)}$	1.01	1.28	2	0.02	0.08	0	0.12	0.15
$v \sin i$ (km s^{-1})	84	60	>300	132	87	28	5	77
$v_{\rm rad}$ (km s^{-1})	−91	+34	∼−140	+7	+26	−8	+20	+14
Observed at:								
S/N	205	200	88	274	387	390	228	214
Airmass (Sec z)	1.07	1.11	1.03	1.46	1.70	1.12	1.36	1.03

with its comparable rotation and spectral type to BD+63° 1964 was used as the main stellar standard. HD 205021, a slow rotator, further enabled us to control the identification of stellar lines in BD+63° 1964. HD 32630 was used as a telluric standard.

BD+63° 1964, is a B0 II star and has therefore relatively few stellar lines. Nevertheless the spectrum has, especially towards the blue, some prominent stellar lines which hamper the detection and measurement of possible new DIBs. Few stellar lines appear above 4800 Å where most of the diffuse interstellar bands are concentrated. To distinguish DIBs from stellar lines the spectrum of BD+63° 1964 was divided by the stellar standard HD 37128, which is a very good match in spectral type and rotational velocity. The resulting spectrum is characterised mostly by interstellar features, with a few residual stellar lines.

Telluric contamination limits the detection and measurement of DIBs and affects a significant fraction of our total wavelength range. The contamination is due to oxygen lines, mostly around the diffuse band at 6284 Å and water lines above 5800 Å. Although the oxygen column density remains stable throughout the observations, the H_2O column density can vary slightly between exposures. For telluric correction the bright star HD 32630 was chosen. To remove the atmospheric contamination the relation below is used:

$$I_{\rm TC} = \frac{I}{I_{\rm t}^{\frac{z}{z_t}}}$$

I and $I_{\rm t}$ are the object spectrum and the telluric standard spectrum respectively. $\frac{z}{z_t}$ is the ratio of the respective airmasses. The inaccuracy in airmass estimations usually requires some iterations to obtain the true ratio. In removing stellar lines from regions contaminated by telluric absorption, both BD+63° 1964 and HD 37128 were first divided by HD 32630.

The heavily reddened star BD+40° 4220 ($E_{(B-V)}$=2) and HD 183143 ($E_{(B-V)}$=1.28), up to now the reference star for studies of DIB behaviour, were used to add confirmation to the newly detected DIBs in this present survey. HD 183143, a B7 star, has been used in previous DIB surveys (Herbig 1975; Jenniskens & Désert 1994; Herbig 1995). BD+40° 4220 is a hot star (spectral type O7) with a fast rotation which is ideal for detecting weak DIBs, especially in the visible and infrared. HD 164353 was used to identify stellar lines and remove telluric contamination in HD 183143, and HD 188209 was used as BD+40° 4220's telluric standard. Due to slight reddening in the standards HD 164535 and HD 188209, the large DIBs at 6284 Å and 6283 Å in these stars incurred an additional error of ∼10%. See Fig. 40 for samples of corrected and uncorrected telluric contamination in the target stars.

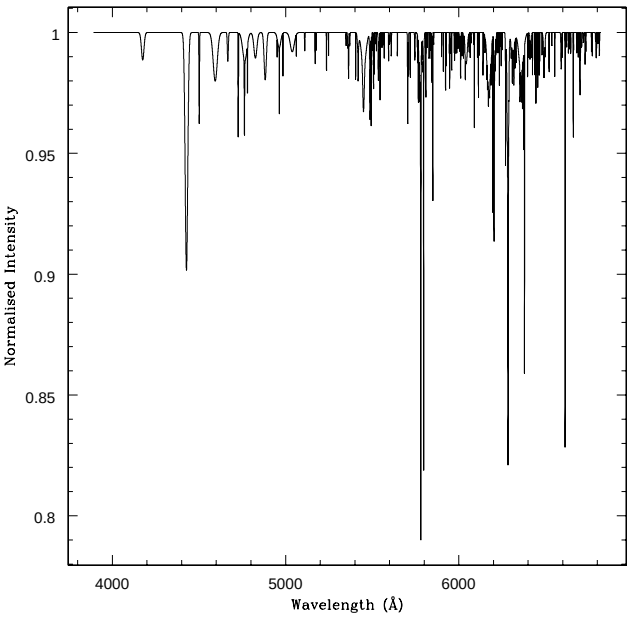

Fig. 1. A synthetic spectrum of all 226 DIBs confirmed towards BD+63° 1964 between 3906 Å and 6812 Å

4. DIB measurement methods

Central wavelengths, equivalent widths and full widths at half maximum were measured in the spectra of the three reddened stars (BD+63° 1964, BD+40° 4220, and HD 183143) using the IRAF (**I**mage **R**eduction and

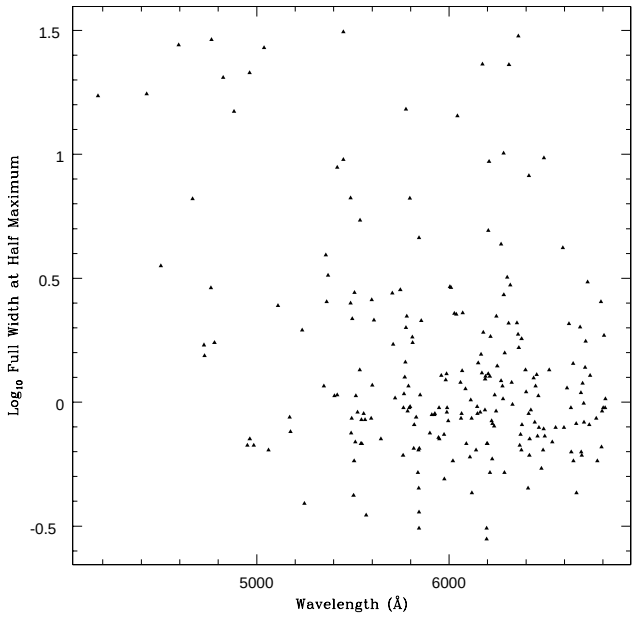

Fig. 2. A plot of $\mathrm{Log}_{10}(FWHM)$ against wavelength for the DIBs measured toward BD+63° 1964. A dominant population of DIB widths lies between 0.6 and 1.4 Å, more abundant towards the red and clustered around some ranges. A second population of medium-broad DIBs is apparent with $FWHM$ between 1.4 and 3.2 Å. It also illustrates the clustering of some DIBs around "magic" wavelengths, at 550, 580 and 630 nm

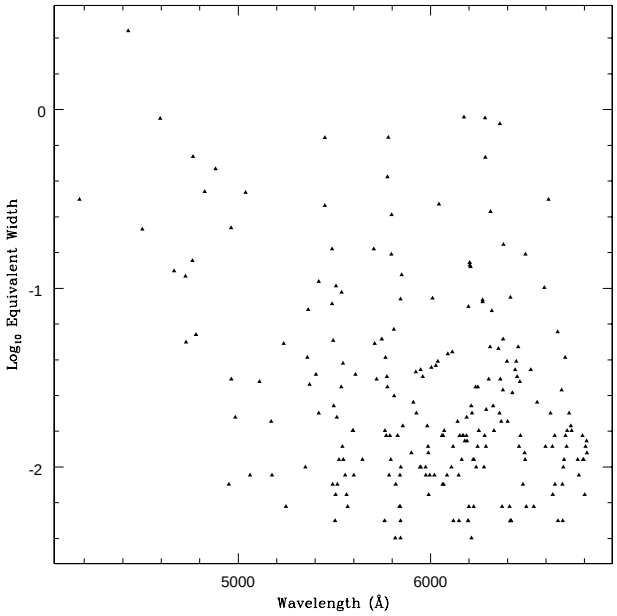

Fig. 4. A plot of $\mathrm{Log}_{10}(EW)$ against wavelength for the DIBs measured toward BD+63° 1964. This plot illustrates the increased number of DIBs detected for a given equivalent width towards the red, and the clustering of DIBs around 550, 580, and 630 nm

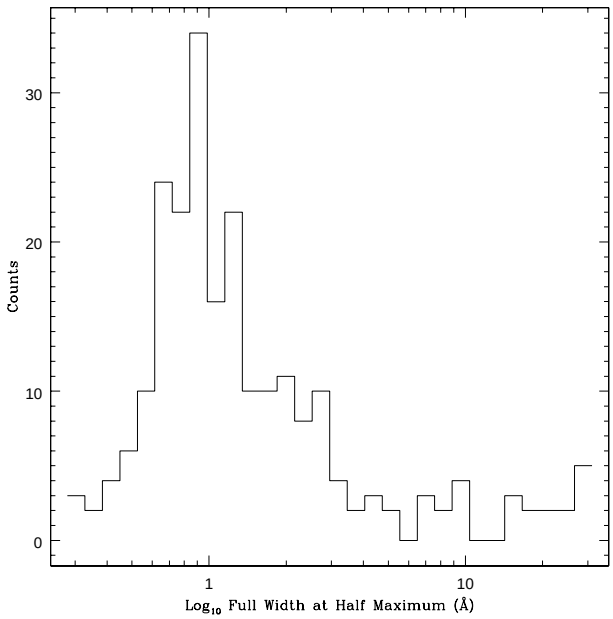

Fig. 3. Histogram of Full Widths of DIBs in BD+63° 1964. This plot illustrates the three populations of DIBs discussed in the text: narrow DIBs, medium broad DIBs and broad DIBs

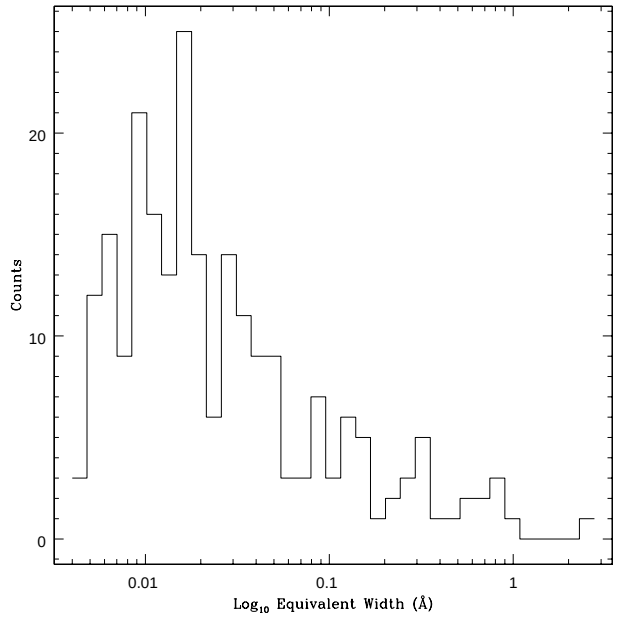

Fig. 5. Histogram of Equivalent Widths of DIBs in BD+63° 1964. The cut off at $\sim$ 5 mÅ corresponds to the sensitivity limit for confident detection

Analysis **F**acility) software package. Equivalent widths were obtained by integration of the pixel intensities within the region:

$$W = \sum_i \left(1 - \frac{I_i}{C_i}\right)$$

where I_i is the intensity at pixel i and C_i is the continuum level at pixel i. The central wavelength was estimated by calculating:

$$\lambda_c = \frac{\sum_i \lambda_i (I_i - C_i)^{\frac{3}{2}}}{\sum_i (I_i - C_i)^{\frac{3}{2}}}$$

where λ_i is the wavelength of pixel i. Alternatively a Gaussian profile can be fitted to the feature, resulting in the additional estimation of the full width at half maximum. Accurately defining the continuum level, which is especially important in measuring medium-broad to broad DIBs, involves fitting a polynomial to the continuum and dividing it out of the spectrum.

Error estimates, using a model based on the Poisson statistics of the data, were also obtained using the IRAF package. An error estimate model is fit to the data using as input a constant σ estimated from the statistics of the spectrum. A number of simulations are created in which random Gaussian noise is added to the noise-free spectrum using the pixel sigmas from the noise model. The model fitting is done for each simulation and the absolute deviation of each fitted parameter to the noise-free model parameter is recorded. The error estimate for each parameter is then calculated as that deviation, inside which contains 68.3% (1 σ) of the parameter estimates.

The wavelengths of absorption bands of certain known molecular, atomic and ionic species (Ca II, Ca I, CH and CH^+) residing in the line of sight towards BD+63° 1964 were measured and the shift in wavelength between those lines and their values recorded in the laboratory was calculated. The sodium lines at 5890 Å and 5895 Å were saturated and so were not included in these calculations. Under ideal conditions the velocity shift would be identical for all lines. However the presence of at least two main clouds of similar column densities and of different velocities (the velocity difference between two substructures in the molecular absorption line was measured to be ∼8 km s^{-1}) in the line of sight of BD+63° 1964 and the resulting two-component structure of the interstellar lines limited the estimation of the correct wavelength to an accuracy of ∼0.05 Å. The average central wavelengths of the interstellar lines were measured and an average of the velocity shift of 19.5 ± 0.5 km s^{-1} was obtained based upon these measurements. The DIBs' measured wavelengths were then shifted by this amount to provide reliable laboratory wavelengths.

5. Selection criteria for new DIBs

Despite the high quality of BD+63° 1964's spectrum, the presence of weak spurious absorption features, including uncorrected or poorly corrected bad pixels and cosmic rays, atmospheric residuals left after the telluric correction and mismatches in stellar abundances between BD+63° 1964 and HD 37128, results in the need for strong and consistent criteria for the positive identification of new DIBs. We checked that new DIBs could not be ascribed to such spurious features.

5.1. The standard stars and synthetic stellar spectrum

Although standard stars HD 37128 and HD 205021 were used to identify and eliminate stellar lines from our target spectrum, we have additionally produced a synthetic spectrum using the TLUSTY and SYNSPEC software (a stellar atmospheres model and emergent line synthesis package) to confirm the DIB identification.

The synthetic stellar spectrum together with the spectra of the standard stars HD 205021 and HD 37128 allowed the identification of stellar lines to very good accuracy in the star BD+63° 1964. Some residual absorption in the divided spectrum which coincided exactly in wavelength with strong or moderate stellar lines together with a band width comparable to the rotational velocity of BD+63° 1964 were ascribed to slight mismatches in stellar abundances between HD 37128 and BD+63° 1964 and thus were not due to bona fide DIBs in the line-of-sight.

5.2. The presence of new DIBs in other reference targets

The most important test of new DIBs are their occurence in other well known reddened stars. The large number of DIBs detected toward BD+63° 1964 may be exceptional and some DIBs might possibly only be observed in such hot and heavily reddened targets. Nevertheless the considerable strength of several DIBs suggested they might be visible in other stars. As previously mentioned HD 183143 and BD+40° 4220 were chosen as our DIB reference targets. The latter was selected due to its very reddened line-of-sight, and HD 183143 is a well known DIB source and a main target of the DIB survey by Jenniskens & Désert (1994) and Herbig (1995). HD 183143 (spectral type B7 I) suffers from some stellar line contamination and BD+40° 4220 (spectral type O7) has a faint visible magnitude of 9.05. For BD+40° 4220 we could therefore obtain a spectrum with a signal-to-noise ratio of only 88 in V but rising to 170 in the red.

All new DIB candidates were cross checked against these spectra and, after eliminating the possibility of stellar line contamination, 60 of these DIB candidates were confirmed in the spectrum of either HD 183143 or BD+40° 4220. Only those DIBs visible in either BD+40° 4220 or HD 183143 along with BD+63° 1964 were included in Table 4.

6. Results

6.1. Spectral displays and table

Figures 6 to 39 display the ELODIE echelle spectral orders of BD+63° 1964, BD+40° 4220 and HD 183143 over the wavelength range 3906 − 6812 Å. BD+63° 1964's associated standard stars, HD 205021 and HD 37128, are also shown for the identification of stellar lines. BD+63° 1964's telluric standard, HD 32630, is shown in a separate box. Also plotted is the spectrum of BD+63° 1964 corrected for stellar lines (divided by HD 37128). A synthetic spectrum of all DIBs seen in this survey of BD+63° 1964 is also included to easily identify confirmed DIBs. When necessary, a telluric correction was applied. This is indicated in the figure caption. Table 4 lists all the diffuse interstellar bands positively identified toward BD+63° 1964.

6.2. New DIBs

The 60 new DIBs discovered in BD+63° 1964 do not seem to adhere to any general pattern. They are spread throughout the spectrum, although occasionally clusters of new DIBs arise, and a slight bias can be seen towards the red end of the spectrum. The wavelength range between 6140 Å and 6200 Å is an example of a region with many new weak DIBs blended with the very broad 6173 Å DIB. The vast majority of the new DIBs are weak, narrow features, although some medium-broad DIBs are also reported. This is probably because the ELODIE spectrograph is not suited for the detection of very broad DIBs due to each order's relatively narrow wavelength coverage and the difficulty in merging adjacent orders. Few new DIBs are seen at shorter wavelengths. There are three reasons that could account for this:

- The spectrograph is not as sensitive at shorter wavelengths, where the reddened target is fainter. The noise level is much higher, especially at the beginning of each order;
- The blue range is also dominated by stellar lines, which does not ease a DIB search in that region;
- There are fewer DIBs at a given equivalent width in this wavelength region. DIBs are undoubtedly concentrated towards the red end of the spectrum (this is discussed further in Sect. 7).

6.3. Undetected DIBs mentioned in previous surveys

Some DIBs previously identified in other surveys were not included in the list of DIBs identified in BD+63° 1964's spectrum. Some appeared to be completely absent, or not rising above the noise level of the spectrum. Others were so weak that, taking into account flat-fielding deviations and other spurious absorptions, the absolute confirmation of these features as DIBs was not possible from our data. Certain very broad DIBs extending over wavelength regions which span two or more orders have been omitted due to the insufficient quality of order merging.

Table 2. Previously reported Diffuse Interstellar Bands that could not be detected or reliably measured in BD+63° 1964 and which are not included in the present survey of DIBs. "+" and "o" denotes the classification of certain and probable DIBs according to Jenniskens & Désert (1994). "?" denotes Krelowski's "doubtful" DIBs. The second column lists the DIB central wavelength quoted by the references given. The next two Col. contain data on these DIBs quoted from measurements by Jenniskens at http://www-space.arc.nasa.gov/~leonid/DIBcatalog.html. The fourth column (EW) shows upper limits as measured in our spectrum of BD+63° 1964 to be compared with Col. 2. See Table 4 for Reference codes

	λ_c (Å)	$\frac{W}{E_{(B-V)}}$ (mÅ)	FW (Å)	EW (mÅ)	Comments	Ref.
+	4066.0	283	15	..	Stellar?	He95
+	4880.4	22	1.35	<8	Weak	JD94
o	5845.4	4	0.7	..	Blend DIB	J96
o	5847.7	2	0.61	..	Absent	J96
+	5850.2	6	1.5	..	Blend DIB	J96
o	5902.8	7	1.2	<6	Absent	K95
+	5904.6	9	0.17	<6	Absent	K95
o	5908.3	3	0.6	<8	Weak	K95
o	5927.5	11	0.7	<6	Very Weak	K95
o	5929.6	7	0.6	..	Absent	K95
?	5941.7	-	-	<6	Absent	K95
?	5989.4	-	-	9	Probable	K95
?	5999.8	6	0.6	<8	Weak	K95
o	6032.9	5	0.6	..	Absent	K95
+	6212.7	14	1.23	..	Absent	Ch85
?	6238.8	-	-	<6	Absent	K95
o	6321.5	16	1.45	<6	Absent	JD94
+	6451.6	403	25.4	..	Absent	JD94
o	6494.9	23	1.39	<6	Absent	JD94
+	6532.1	664	17.2	..	too broad	JD94
?	6635.3	-	-	<8	Weak	K95
?	6649.8	-	-	<8	Very Weak	K95
?	6693.3	5	0.8	<6	Blend DIB	K95
?	6696.8	-	-	<6	Absent	K95
+	6741.0	13	0.97	..	too broad	He75
o	6767.6	8	0.7	<8	Weak	He88
o	6768.6	5	0.7	<6	Absent	He95
o	6779.0	3	0.54	<8	Weak	He95

Table 2 shows a list of these suggested DIBs not included in the present survey. Seven of those diffuse interstellar bands denoted "certain" by Jenniskens & Désert (1994) cannot be accurately measured in the present spectrum of BD+63° 1964. The 6741 Å DIB lies between two orders and is therefore lost in our data. Another DIB at 6532 Å spans two orders. We cannot exclude the possiblity of imperfect merging in this case due to the nearby strong

Table 3. Possible additional Diffuse Interstellar Bands in BD+63° 1964. These DIBs have yet to be confirmed. Central wavelength, equivalent width (EW) and full width at half maximum ($FWHM$) are listed

$\lambda_{\rm DIB}$ (Å)	EW (Å)	$FWHM$ (Å)	$\lambda_{\rm DIB}$ (Å)	EW (Å)	$FWHM$ (Å)
4968.87	65	6.54	5724.87	6	0.55
4979.28	14	1.29	5806.52	15	1.54
5098.84	5	0.48	5834.54	9	0.84
5166.33	7	0.68	5966.11	8	0.84
5167.28	8	0.69	6095.21	5	0.65
5176.67	34	3.50	6102.48	12	1.77
5428.63	12	1.11	6154.57	8	1.22
5443.22	7	0.72	6293.29	5	0.41
5525.48	8	0.74	6468.45	9	1.29
5539.73	14	1.48	6476.81	5	0.55
5559.93	6	1.06	6639.34	11	1.11
5632.81	6	0.65	6808.36	7	0.56
5634.73	7	0.89			

H-α line. The absence of a third DIB, at 6451 Å, could possibly be due to its extension over two orders. This DIB however is not visible even when an optimal merging of the orders is obtained. The rest of the "certain" DIBs, except for one, are either too weak to be accurately measured or else absent from the spectrum. The remaining one, at 5850.2 Å, positively identified by Jenniskens et al. (1996), is absent because the resolution of the ELODIE spectrograph, at 42 000, is not sufficient to distinguish this very weak DIB from the stronger and broader band at 5849.8 Å. It was detected with the AURELIE spectrograph at Observatoire d'Haute Provence, France, which has a resolution in excess of 50 000 (Jenniskens et al. 1996). Alternatively this is just a red wing of the 5849.8 Å DIB. All the remaining DIBs not included in the survey have previously been classified as either probable or doubtful.

6.4. Possible additional DIBs to be confirmed

The spectrum of BD+63° 1964 provides us with a unique opportunity for finding and measuring new diffuse interstellar bands. The fact that previously known narrow DIBs are enhanced by a factor of $1.5-3$ toward this target lends credence to this. An absorption band has to fulfill certain criteria as mentioned in Sect. 5 before it can be considered as a new DIB.

The wealth of interstellar features in BD+63° 1964's spectrum has resulted in the discovery of 60 new "certain" DIBs based upon these criteria. There seems to be no doubt that this number is limited by the signal to noise of the present data and the magnitude $V = 8.6$ for this exceptional target. However this seems one of the best targets for DIB surveys when studied with cross-dispersed echelle spectrographs on 2 m class telescopes. It is likely that an analysis of more spectra of higher quality and using a larger telescope would result in the positive detection of many more diffuse bands. In searching BD+63° 1964's spectrum for new DIBs a number of weak absorption features which are probably of interstellar origin were listed. They did not fulfill the necessary criteria to be included as "certain" DIBs in this particular survey. In some cases the uncertainty was due to blended stellar lines or atmospheric lines, or stellar lines in HD 205021 at the wavelength corresponding to that of the suspect DIB coinciding with stellar lines in the synthetic stellar spectrum. In other cases it was difficult to distinguish the feature from localised random noise. Table 3 lists these possible DIBs.

The interest of the present survey comes from the exceptional quality of the spectrum of the line-of-sight of BD+63° 1964, with additional confirmation provided by spectra of the very reddened targets HD 183143 (a B7 star with a slow rotation) and BD+40° 4220 (a hot O7 star with a fast rotation). Due to the unusual enhancement of DIBs in BD+63° 1964 we could not confirm the existence of 25 possible DIBs in the other targets. To confirm or reject these possible DIBs one needs to observe higher signal-to-noise spectra of reddened stars. Those DIBs listed as possible could then be cross-checked with other stars.

7. Statistics on the DIB population

7.1. DIB distribution vs wavelength

In the previous section we discussed the identification of 226 diffuse interstellar bands in the line-of-sight of BD+63° 1964 with added confirmation in two other reddened reference targets and the possible detection of a number of others. Figures 2 and 4 show the distribution of both full widths and equivalent widths of all certain DIBs in the wavelength range of the survey. The blue end of the spectrum is characterised by both a lack of narrow DIBs and an increased abundance of broad DIBs. We rule out the possibility that this could be an instrumental bias. The lower sensitivity and increased abundance of stellar lines in the blue have already been discussed. The sensitivity limit for the survey can be estimated from the expression:

$$\sigma_{EW} = \frac{\sqrt{2\Delta\lambda FWHM}}{\frac{S}{N}}.$$

Assuming a Full Width at half maximum of typically 1 Å, for instance, we find that the sensitivity limit in the equivalent width is homogeneous from 4500 Å to 6500 Å. Applying a 5σ confidence level would lead to the detection of DIBs with an equivalent width >12 mÅ. The equivalent width of a DIB is wavelength-dependent,

$$EW \propto Nf\lambda^2$$

where N is the column density of the carrier and f is the oscillator strength (Spitzer 1978). The DIBs in the red are obviously favoured. If constant column density and oscillator strength are assumed, a DIB with an equivalent width of 15 mÅ at 6000 Å would have an equivalent width of 9 mÅ at 4500 Å. This is however not sufficient to explain the lack of narrow DIBs we see in the blue. A physical explanation must be invoked to explain this phenomenon. Possible explanations might be that stronger and sharper fundamental transitions of large molecules occur in the red while secondary transitions in the blue are broadened due to limited lifetimes in excited levels of molecules (intercoupling between vibronic states).

We therefore find that the survey is homogeneously complete with narrow DIBs stronger than 15 mÅ. The broader DIBs are not only concentrated towards shorter wavelengths. There is a second visible group of medium-broad to broad DIBs around 6200 Å. The pattern of DIBs also seems to involve some clustering. Five clusters of narrow DIBs, four of which gather around one or more broader ones, can be seen above 5500 Å.

7.2. Histograms of DIB widths and intensities

Figures 3 and 5 show histograms depicting the spread of both full widths and equivalent widths of DIBs measured in BD+63° 1964. We can distinguish three populations of DIBs according to their $FWHM$. The most abundant are those whose widths lie between 0.6 Å and 1.4 Å (narrow DIBs). Medium-broad DIBs are seen between a width of 1.4 Å and 3.2 Å, and broad DIBs, broader than 3.2 Å do not show any dominant value in the histogram. It is clear that very broad DIBs are not completely surveyed, not only due to their difficulty of detection in echelle orders, but also due to their lower contrast (for a given Equivalent Width), their blend and mutual confusion with other features. However only very clearly defined DIBs would present an interest in terms of identification. The distribution of full widths at half maximum gives direct information on physical properties of the carriers (e.g. molecular rotational contours for narrow DIBs and lifetime broadening for some of the broad DIBs).

The corresponding plot of the equivalent width distribution on the contrary (considering the statistical dispersion) does not show any preferred equivalent width above the sensitivity cut-off. This is because the equivalent width is a product of three variables, the carrier column density, N, the transition oscillator strength, f, and λ^2, which take a wide and continuous range of values, with independent statistics.

8. Conclusions

8.1. New detections and DIB statistics

Figure 1 shows a composite spectrum of all DIBs seen toward the reddened targets in the wavelength range $3906 - 6812$ Å. The detection of 60 new DIBs raised the total number of DIBs to 226 in this line-of-sight, along with 25 possible DIBs awaiting confirmation. A statistical analysis on the DIB population has clarified the presence of three main DIB groups based on their band widths and has illustrated the clustering of DIBs in selected wavelength bands.

8.2. The enhancement of DIBs in BD+63° 1964 vs. other reference targets

This survey of diffuse interstellar bands in the optical range has confirmed earlier reports of the unique nature of BD+63° 1964 compared to other heavily reddened targets, such as HD 183143 and BD+40° 4220 (Ehrenfreund et al. 1997). What mechanism could cause this unusual enhancement in DIB strengths and lead to the identification of many more hitherto undetected DIBs? The Ca II absorption lines at 3933 and 3968 Å, as well as the CH band at 4300 Å seem to indicate at least two clouds of different velocities in the line-of-sight of BD+63° 1964. In order to understand the DIB behaviour, models of diffuse clouds have been performed using information on various atomic and molecular species residing in the line-of-sight toward BD+63° 1964. The models indicate that the line-of-sight toward this target passes through a cloud edge where ultra-violet radiation may trigger the ionization of DIB carriers (Tuairisg et al. 2000). Further modeling and observational efforts are required to constrain the environmental conditions in this exceptional line-of-sight.

8.3. Future work

Higher signal-to-noise spectra of BD+63° 1964 and other reddened targets would undoubtedly confirm many of the possible DIBs listed in Table 3, and possibly lead to the detection of more new DIBs. Important further work would be to complement this work with a comprehensive survey of DIBs in the near infra-red. Observations taken with the INT/MUSICOS spectrograph are currently under analysis. As previously mentioned, the ELODIE spectrograph has limitations for a survey of broader DIBs. Further observations of reddened targets using more suitable spectrographs to detect broad DIBs, are also desirable.

The new survey presented in this paper provides a new basis for comparison with spectroscopic measurements of DIB carrier candidates in the laboratory. However, with the large number of detected DIBs namely ∼200 DIBs

between 5400 and 6800 Å, we find on average one DIB every 6 Å. Therefore any identification in this range based only on wavelength coincidence could be obtained by pure chance and additional criteria for identification are necessary, such as multiple bands, band widths, DIB strength ratios and correlated variations in different environments (Ehrenfreund & Foing 1995; Herbig 1995).

Follow-up studies of the surveyed DIBs by high resolution spectroscopy and the physical properties of the line-of-sight conditions will further help to reveal the nature of DIB carriers.

Acknowledgements. We thank the staff at OHP for their help during the observations. PE is a recipient of an APART fellowship. SÓT acknowledges support for a research stage at ESA Space Science Department.

References

Baranne A., Queloz D., Mayor M., et al., 1996, A&AS 119, 373-390
Beals C.S., Blanchet G.H., 1937, PASP 49, 224
Cami J., Sonnentrucker P., Ehrenfreund P., Foing B.H., 1996, A&A 326, 822
Chlewicki G., 1985, Observational constraints on multimodal Interstellar Grain Populations. Thesis Leiden University
Chlewicki G., Groot M.S., Van der Zwet G.P., Greenberg J.M., Alvarez P.P., Mampaso A., 1987, A&A 173, 131
Ehrenfreund P., Foing B.H., 1995, Planetary Space Sci. 43, 10/11, 1183
Ehrenfreund P., Foing B.H., 1996, A&A 307, L25
Ehrenfreund P., Cami J., Dartois E., Foing B.H., 1997, A&A 318, L28
Ferlet R., Roueff E., Horani M., Rostas J., 1983, A&A 125, L5
Ferlet R., Dennefeld M., 1984, A&A 138, 303
Foing B.H., Ehrenfreund P., 1994, Nat 369, 296
Foing B.H., Ehrenfreund P., 1997, A&A 317, L59
Freivogel P., Fulara J., Maier J.P., 1994, ApJ 431, L151-L154
Hayden-Schmitt W., Snow T.P., Jura M., Cochran W.D.S., 1981, ApJ 248, 128
Heger M.L., 1922, Lick Obs. Bull 10, 146
Herbig G.H., 1966, Zs. f. Astrophys. 64, 512
Herbig G.H., 1967, in: Radio Astronomy and the Galactic System, IAU Symp. 31, van Woerden H. (ed.), p. 85
Herbig G.H., 1975, ApJ 196, 129
Herbig G.H., 1988, ApJ 331, 999
Herbig G.H., 1995, ARA&A 33, 19
Herbig G.H., Leka K.D., 1991, ApJ 382, 193
Hobbs L.W., 1984, ApJ 280, 132
Jenniskens P., Désert X., 1993, A&A 274, 465
Jenniskens P., Désert X., 1994, A&AS 106, 39
Jenniskens P., Porceddu I., Benvenuti P., Desert F.-X., 1996, A&A 313, 649-656
Krelowski J., Sneden C., Hiltgen D., 1995, Planetary and Space Sci. 43, 1195-1203
Merrill P.W., 1934, PASP 46, 206
Salama F., Bakes E.L.O., Allamandola L.J., Tielens A.G.G.M., 1996, ApJ 458, 621
Sanner F., Snell R., Vanden Bout P., 1978, ApJ 226, 460
Sarre P.J., Miles J.R., Kerr T.H., Hibbins R.E, Fossey S.J., Somerville W.B., 1995, MNRAS 277, L41
Sorokin P., Glownia J.H., 1996, ApJ 473, 900
Spitzer L., 1978, Physical Processes in the Interstellar Medium. Wiley, New York
Tulej M., Kirkwood D.A., Pachkov M., Maier J.P., ApJ 506, L69-L73
Tuairisg S.Ó., Spaans M., Ehrenfreund P., Foing B.H., 2000 (in preparation for A&A)
Ubachs W., Hinnen P.C., Reinhold E., 1997, ApJ 476, L93
Wilson R., 1958, ApJ 128, 57

Table 4. Confirmed Diffuse Interstellar Bands measured towards BD+63° 1964, HD 183143 and BD+40° 4220. The first Col. (λ) gives the central absolute wavelength (in air) after correcting for the cloud velocity shift. EW denotes the diffuse band equivalent width measured in the spectra of the reddened targets (tellurically corrected where necessary, as indicated in Fig. 6 through to Fig. 39). Errors for these values are denoted Err_{EW}. $FWHM$ denotes the full width at half maximum of the DIBs. Errors for these values are denoted Err_{FWHM}. The final Col. (*Ref.*) cites the source of the first identification of the DIB in other targets. New DIBs are denoted by "New". Due to BD+63° 1964's $E_{(B-V)}$ of 1.01 normalisation to unit reddening is not necessary. DIBs which could not be measured due to stellar line contamination are marked with an asterisk (*). A horizontal line denotes the absence of a DIB in the spectrum. Reference codes are: Hg22 - Heger (1922), Me34 - Merrill (1934), BB37 - Beals & Blanchet (1937), Wi58 - Wilson (1958), He66 - Herbig (1966), He67 - Herbig (1967), He75 - Herbig (1975), Sa78 - Sanner et al. (1978), HS81 - Hayden-Schmitt et al. (1991), F83 - Ferlet et al. (1983), FD84 - Ferlet & Dennefeld (1984), Ho84 - Hobbs (1984), Ch85 - Chlewicki (1985), Chl87 - Chlewicki (1987), He88 - Herbig (1988), HL91 - Herbig & Leka (1991), JD93 - Jenniskens & Désert (1993), JD94 - Jenniskens & Désert (1994), K95 - Krelowski et al. (1995), J96 - Jenniskens et al. (1996)

λ	EW	Err_{EW}	EW	Err_{EW}	EW	Err_{EW}	$FWHM$	Err_{FWHM}	Ref.
(Å)	(mÅ)	(mÅ)	(mÅ)	(mÅ)	(mÅ)	(mÅ)	(Å)	(Å)	
	BD+63° 1964		HD 183143		BD+40°4220				
4175.46	314	81	450	95	—	—	17.2	5.22	JD94
4427.96	2760	120	2470	100	2236	250	17.5	1.24	BB37
4501.65	214	10	160	22	127	60	3.55	0.16	He66
4593.93	891	45	545	150	780	110	27.6	2.21	JD94
4666.65	125	7	54	10	—	—	6.61	0.38	JD94
4726.35	117	7	107	6	204	43	1.70	0.08	He75
4728.35	50	4	41	5	74	23	1.54	0.12	He75
4762.57	143	5	140	5	76	7	2.89	0.16	He75
4764.66	546	55	450	109	1020	250	29.0	3.56	He75
4780.10	55	4	53	3	59	5	1.74	0.22	He75
4825.94	347	27	377	65	—	—	20.4	2.17	JD94
4882.56	466	20	950	60	1900	350	14.9	0.76	Wi58
4951.05	8	2	6	2	5	2	0.67	0.11	New
4963.03	218	12	239	110	540	200	21.3	2.70	JD94
4963.89	31	3	24	2	54	4	0.71	0.08	JD94
4984.78	19	2	8	3	14	3	0.67	0.16	JD94
5038.59	344	33	421	105	541	150	26.9	2.50	JD94
5061.56	9	2	10	2	10	5	0.64	0.15	New
5110.81	30	6	45	10	35	16	2.45	0.51	JD94
5170.69	18	3	*	*	10	50	0.87	0.18	New
5176.00	9	2	11	2	13	4	0.76	0.20	New
5236.34	49	3	51	23	34	7	1.95	0.10	New
5247.91	6	3	6	2	22	8	0.39	0.20	New
5349.16	10	3	8	2	15	3	1.16	0.47	New
5359.58	41	9	52	11	55	10	3.92	0.77	He67
5363.78	76	7	124	10	130	20	2.54	0.24	JD94
5370.36	29	4	11	3	15	5	3.25	0.61	New
5404.52	33	2	41	2	30	4	1.06	0.08	He75
5418.39	109	9	89	12	—	—	8.85	0.39	He75
5419.05	20	2	12	3	25	5	1.07	0.11	New
5449.76	290	12	345	34	242	40	9.53	0.50	He75
5450.95	696	22	444	150	619	100	31.2	1.46	JD94
5487.54	82	8	67	4	111	20	2.51	0.32	He75
5487.90	166	12	117	15	190	50	6.67	0.54	JD94

Table 4. continued

λ (Å)	EW (mÅ)	Err_{EW} (mÅ)	EW (mÅ)	Err_{EW} (mÅ)	EW (mÅ)	Err_{EW} (mÅ)	$FWHM$ (Å)	Err_{FWHM} (Å)	Ref.
	BD+63° 1964		HD 183143		BD+40°4220				
5490.52	8	2	7	2	7	3	0.75	0.19	New
5494.10	51	3	30	2	27	3	0.86	0.07	He75
5497.00	22	5	17	4	17	5	2.17	0.90	New
5503.16	5	2	8	2	< 14	7	0.42	0.15	New
5506.06	7	2	*	*	11	3	0.58	0.24	New
5508.03	103	6	121	16	108	11	2.77	0.36	He75
5512.66	19	2	8	2	15	3	0.69	0.07	New
5515.97	8	3	7	2	8	3	1.06	0.35	New
5524.47	11	2	< 8	4	13	4	0.91	0.24	JD94
5535.26	28	4	40	4	42	5	1.35	0.13	JD94
5537.51	95	18	85	11	100	20	5.42	0.29	He75
5541.78	13	3	5	2	11	2	0.68	0.21	JD94
5545.02	38	4	30	2	27	3	0.85	0.09	He75
5546.52	11	3	< 8	4	7	2	0.68	0.17	New
5556.27	9	3	12	2	7	3	0.90	0.31	New
5563.06	7	3	< 8	4	8	3	0.85	0.30	New
5569.08	6	2	7	2	9	3	0.35	0.16	New
5594.54	16	3	10	2	16	3	0.86	0.15	New
5597.38	16	4	5	2	8	4	2.59	1.01	New
5600.49	9	2	9	2	7	3	1.17	0.39	New
5609.96	33	6	23	3	50	7	2.14	0.57	JD94
5645.43	11	2	*	*	16	3	0.71	0.15	New
5705.10	166	10	163	10	214	24	2.75	0.12	He67
5709.40	49	9	29	3	43	5	1.71	0.27	JD94
5719.68	31	4	25	3	24	3	1.04	0.20	JD94
5746.21	52	4	48	5	35	4	2.84	0.20	JD94
5760.64	5	3	< 8	4	6	2	0.61	0.13	K95
5762.80	16	3	8	2	< 12	6	0.95	0.11	JD93
5766.17	41	3	21	3	29	4	1.08	0.07	Ch87
5769.32	15	2	12	3	18	3	1.26	0.28	JD93
5772.67	32	3	24	3	44	5	1.45	0.14	JD93
5776.13	420	31	640	39	501	32	15.2	2.20	Hg22
5776.21	28	4	19	4	29	4	2.00	0.30	JD93
5780.55	699	4	770	8	713	11	2.22	0.01	Hg22
5784.86	9	2	11	2	15	5	0.92	0.36	JD93
5789.04	15	3	20	2	52	6	1.16	0.15	JD93
5793.13	11	2	5	2	9	3	0.95	0.19	K95
5796.07	155	16	138	18	236	30	6.65	0.70	He67
5797.08	258	15	187	10	179	7	0.96	0.05	Hg22
5809.53	59	7	26	3	*	*	1.83	0.25	JD94
5810.21	25	7	10	2	*	*	1.74	0.30	JD93
5815.80	4	2	< 8	4	8	3	0.65	0.27	JD93
5818.47	8	3	22	2	13	3	0.81	0.32	JD93
5828.56	15	2	12	2	22	3	0.87	0.16	JD93
5837.92	6	2	18	2	6	3	0.52	0.28	J96
5840.62	9	3	< 8	4	< 8	4	0.64	0.23	J96
5842.38	6	2	< 4	4	< 4	4	0.45	0.20	J96
5843.30	5	3	< 8	4	< 8	4	0.36	0.10	J96
5843.69	4	3	< 8	4	< 8	4	0.31	0.15	J96
5844.28	87	11	132	12	111	14	4.61	0.59	He67
5844.95	10	3	12	2	< 8	4	0.65	0.21	JD94
5849.81	119	2	62	4	84	4	1.07	0.01	He67

Table 4. continued

λ (Å)	EW (mÅ)	Err_{EW} (mÅ)	EW (mÅ)	Err_{EW} (mÅ)	EW (mÅ)	Err_{EW} (mÅ)	$FWHM$ (Å)	Err_{FWHM} (Å)	Ref.
	BD+63° 1964		HD 183143		BD+40°4220				
5854.85	17	5	19	3	15	4	2.13	0.67	JD94
5900.58	12	3	12	2	16	3	0.75	0.16	K95
5910.54	23	3	< 14	7	23	4	0.89	0.09	K95
5923.51	34	3	23	3	33	3	0.89	0.16	K95
5925.81	20	3	19	2	17	3	0.90	0.13	K95
5945.53	10	2	10	2	15	5	0.72	0.24	K95
5947.29	35	3	16	2	19	3	0.95	0.09	K95
5948.87	10	3	6	2	< 8	4	0.71	0.20	K95
5958.89	32	3	52	7	30	4	1.28	0.08	New
5973.78	10	2	8	2	16	4	0.74	0.13	New
5975.66	9	2	< 8	4	5	2	0.49	0.08	K95
5982.77	17	3	16	2	7	3	1.23	0.18	He75
5986.60	13	3	6	2	< 8	4	1.30	0.29	K95
5988.04	12	3	12	2	5	2	0.91	0.13	K95
5989.51	7	2	6	2	5	2	0.95	0.24	K95
5995.73	9	4	7	2	7	3	0.84	0.31	K95
6004.80	36	3	30	3	15	3	2.92	0.38	HL91
6010.48	88	4	105	7	129	7	2.90	0.15	He75
6019.45	9	2	17	2	24	3	0.58	0.11	JD94
6027.09	37	4	35	4	45	4	2.28	0.25	JD94
6037.47	39	3	33	4	78	8	2.26	0.19	JD94
6042.84	296	32	262	23	367	40	14.3	3.33	He75
6059.88	15	5	9	2	20	4	1.20	0.50	JD94
6061.52	8	4	7	2	< 8	4	0.86	0.34	New
6065.19	15	3	15	2	15	3	0.90	0.17	JD94
6068.45	8	3	6	2	10	3	1.34	0.25	New
6071.08	16	5	16	3	52	20	2.29	0.98	JD94
6084.94	9	2	10	3	10	2	1.13	0.36	New
6089.79	43	2	24	3	23	3	0.68	0.03	HL91
6108.14	10	2	11	2	10	3	0.60	0.15	JD94
6113.20	44	3	43	3	25	3	1.02	0.04	He75
6116.74	13	2	14	2	15	2	0.86	0.08	JD94
6118.66	5	2	5	2	8	3	0.43	0.10	New
6139.94	18	2	23	3	22	3	0.64	0.03	JD94
6145.41	9	9	< 8	4	< 12	6	0.96	0.25	New
6147.02	5	2	*	*	15	4	0.90	0.32	New
6151.15	15	2	*	*	10	3	1.44	0.20	New
6161.83	11	2	8	2	11	2	0.91	0.13	New
6165.72	15	3	10	2	7	2	1.56	0.23	New
6170.71	15	3	17	3	9	3	1.31	0.17	New
6173.65	907	22	1059	120	1075	81	23.1	1.24	Wi58
6177.72	14	3	8	2	10	3	1.91	0.48	New
6185.89	15	3	9	2	11	3	0.93	0.15	New
6187.19	19	3	10	2	10	3	1.24	0.22	New
6189.31	14	3	7	2	15	3	1.27	0.20	JD94
6194.57	5	2	6	2	6	3	0.31	0.08	HS81
6194.98	5	2	5	2	7	2	0.28	0.04	JD94
6195.99	79	3	86	5	66	3	0.68	0.03	He67
6198.82	6	3	11	3	< 18	9	0.68	0.23	JD94
6203.06	139	13	125	18	124	22	1.30	0.03	He67
6204.22	135	9	123	9	143	20	4.92	0.51	He67
6207.52	132	17	160	17	150	30	9.34	1.47	JD94
6211.74	22	2	9	2	14	3	1.27	0.17	K95

Table 4. continued

λ (Å)	EW (mÅ)	Err_{EW} (mÅ)	EW (mÅ)	Err_{EW} (mÅ)	EW (mÅ)	Err_{EW} (mÅ)	$FWHM$ (Å)	Err_{FWHM} (Å)	Ref.
	BD+63° 1964		HD 183143		BD+40°4220				
6212.95	4	2	5	2	10	3	0.52	0.19	Ch85
6215.80	20	3	13	2	22	4	1.84	0.44	JD94
6220.86	11	3	7	3	11	4	0.84	0.27	K95
6223.53	6	2	10	2	5	2	0.59	0.18	JD94
6226.02	11	2	6	2	11	3	0.82	0.12	K95
6234.01	28	4	18	3	12	2	0.80	0.15	He75
6236.71	10	4	9	2	9	3	1.07	0.42	JD93
6244.42	13	4	22	3	6	2	0.92	0.12	New
6245.36	28	3	22	4	20	7	2.22	0.71	K95
6250.77	16	3	8	3	10	3	1.40	0.32	New
6269.82	84	5	115	10	100	9	1.22	0.10	He67
6270.45	86	11	130	11	128	17	4.34	0.91	He75
6278.17	10	5	32	5	28	5	1.16	0.57	JD93
6280.48	15	5	10	2	17	4	1.03	0.37	JD93
6283.30	899	45	1240	102	1172	120	10.1	0.12	JD93
6284.09	540	11	689	19	712	20	2.71	0.06	Me34
6287.57	13	4	12	2	7	2	0.52	0.24	JD93
6289.70	21	6	20	3	18	5	1.58	1.00	JD93
6302.29	31	3	20	3	30	4	3.19	0.39	New
6308.92	47	3	78	10	90	20	2.08	0.09	HL91
6311.53	268	32	390	48	230	120	23.0	2.64	He75
6317.75	75	11	60	7	139	22	2.97	0.19	JD93
6324.81	22	6	22	2	17	3	1.20	0.26	JD93
6330.14	16	2	18	3	28	10	0.98	0.15	JD93
6353.18	46	3	38	3	30	3	2.09	0.12	He75
6358.54	20	3	15	2	18	3	1.88	0.22	New
6360.21	834	55	920	200	830	125	30.0	2.50	HL91
6362.23	31	4	32	2	29	6	1.66	0.21	HL91
6367.28	18	2	18	2	12	3	0.67	0.09	Ho84
6371.92	6	3	*	*	11	2	0.74	0.29	K95
6376.02	27	4	44	4	38	4	0.64	0.09	He75
6376.57	52	7	20	4	54	6	1.80	0.29	JD94
6379.22	176	3	107	3	85	4	0.81	0.01	He75
6396.95	39	3	55	4	37	5	1.35	0.12	HL91
6400.37	18	2	12	2	6	3	1.10	0.11	K95
6410.08	6	2	< 8	4	7	3	0.45	0.14	New
6414.15	5	3	22	2	6	3	0.90	0.25	HL91
6414.76	89	9	130	22	174	25	8.20	1.05	HL91
6417.27	5	2	8	2	< 14	7	0.61	0.19	New
6418.54	5	2	< 8	4	5	2	0.71	0.18	New
6425.61	26	3	21	2	32	3	0.93	0.10	He67
6439.42	35	3	39	3	22	3	1.25	0.10	HL91
6445.25	39	4	42	3	34	3	0.83	0.11	HL91
6449.30	32	3	21	2	14	3	1.16	0.11	HL91
6456.08	47	3	49	7	62	7	1.29	0.08	New
6460.31	13	3	10	2	< 14	7	0.73	0.34	JD94
6463.63	30	2	23	3	35	5	1.06	0.07	New
6466.95	15	2	12	2	7	3	0.79	0.06	New
6480.48	8	2	< 8	4	28	11	0.54	0.08	New
6489.29	12	3	6	2	< 8	4	0.64	0.08	New
6492.17	11	2	20	2	17	3	0.78	0.15	JD94
6492.92	155	21	135	24	180	30	9.67	1.17	JD94
6497.79	6	3	4	2	11	2	0.73	0.33	JD94
6520.95	35	3	41	3	54	7	1.35	0.10	JD94

Table 4. continued

λ (Å)	EW (mÅ)	Err_{EW} (mÅ)	EW (mÅ)	Err_{EW} (mÅ)	EW (mÅ)	Err_{EW} (mÅ)	$FWHM$ (Å)	Err_{FWHM} (Å)	Ref.
	BD+63° 1964		HD 183143		BD+40°4220				
6536.86	6	3	8	2	22	4	0.69	0.30	JD94
6553.76	23	2	17	3	17	3	0.79	0.05	New
6591.03	101	17	97	4	—	—	4.19	0.46	JD94
6597.47	13	3	20	3	15	3	0.79	0.21	He75
6613.63	314	4	320	4	300	5	1.14	0.01	Me34
6622.59	20	4	18	3	14	3	2.07	0.64	K95
6632.86	13	3	22	3	20	3	0.95	0.29	JD94
6635.50	7	2	7	2	10	2	0.63	0.20	K95
6644.33	15	3	29	3	25	5	1.43	0.26	New
6645.95	8	2	11	2	9	3	0.58	0.20	K95
6660.62	57	3	75	4	51	3	0.82	0.02	JD94
6662.25	5	2	8	2	35	4	0.43	0.12	New
6681.07	27	4	*	*	*	*	2.01	0.18	K95
6684.83	8	3	5	2	*	*	1.09	0.19	New
6686.46	5	2	< 8	4	*	*	0.63	0.13	New
6689.38	10	3	17	2	22	2	0.61	0.17	K95
6694.40	11	2	8	2	10	2	1.19	0.33	JD94
6699.28	41	3	48	2	27	3	0.99	0.07	Sa78
6701.87	15	3	20	2	7	2	0.83	0.13	Fe83
6707.73	13	3	< 8	4	6	2	1.38	0.41	New
6709.65	16	4	13	2	*	*	1.76	0.44	FD84
6719.58	20	3	*	*	11	3	3.05	0.20	New
6729.20	17	2	13	2	14	4	0.81	0.09	New
6733.35	16	2	26	3	< 8	4	1.28	0.17	New
6765.39	11	3	12	2	7	2	0.86	0.19	New
6770.23	9	2	18	2	10	2	0.58	0.12	He75
6789.64	15	3	9	2	10	2	2.54	0.38	He88
6792.54	11	3	19	3	9	2	0.66	0.14	He88
6795.18	11	4	15	2	5	2	0.92	0.33	He88
6801.39	7	3	15	2	12	3	0.95	0.34	He88
6804.82	13	3	7	2	13	3	1.86	0.27	He88
6811.30	14	3	18	3	21	4	0.95	0.23	He88
6812.39	12	3	20	3	12	3	1.03	0.33	He88